Intrinsic spin-orbit coupling in superconducting δ-doped $SrTiO_3$ heterostructures

M. Kim,[1,2] Y. Kozuka,[2,3] C. Bell,[1] Y. Hikita,[1] and H. Y. Hwang[1,4]

[1]*Stanford Institute for Materials and Energy Sciences, SLAC National Accelerator Laboratory, Menlo Park, California 94025, USA*

[2]*Department of Advanced Materials Science, University of Tokyo, Kashiwa, Chiba 277-8561, Japan*

[3]*Department of Applied Physics and Quantum-Phase Electronics Center (QPEC), University of Tokyo, Bunkyo-ku, Tokyo 113-8656, Japan*

[4]*Geballe Laboratory for Advanced Materials, Department of Applied Physics, Stanford University, Stanford, California 94305, USA*

(Received 25 June 2011; revised manuscript received 12 July 2012; published 15 August 2012)

We report the violation of the Pauli limit due to intrinsic spin-orbit coupling in $SrTiO_3$ heterostructures. Via selective doping down to a few nanometers, a two-dimensional superconductor is formed, geometrically suppressing orbital pair breaking. The spin-orbit scattering is exposed by the robust in-plane superconducting upper critical field, exceeding the Pauli limit by a factor of 4. Moreover, transport scattering times several orders of magnitude higher than for conventional thin-film superconductors enable this system to enter a different regime of cleanliness, where intrinsic band spin-orbit coupling effects arise in these symmetrically doped samples.

DOI: 10.1103/PhysRevB.86.085121 PACS number(s): 74.78.−w, 71.70.Ej, 74.25.F−, 74.25.Op

Unconventional superconductivity is a subject of great theoretical and experimental interest.[1–3] A central issue in this field is the discovery and understanding of nontrivial pairing mechanisms, such as the spin-triplet Cooper pair, which has been explicitly investigated in heavy fermions,[1] Sr_2RuO_4,[4] and crystals with broken inversion symmetry.[5] Recently, novel pairing has also been predicted in two-dimensional systems breaking inversion symmetry.[6,7] Experimentally, measurements of the superconducting upper critical field H_{c2} give vital information. In particular, violations of the Pauli paramagnetic limit[8,9] can be used to unravel the nature of the electron spins in the superconducting state. Notably, the presence of spin-orbit coupling (SOC) can be quantified,[10] as demonstrated by the H_{c2} studies of metal thin-film superconductors[11] and bilayer systems where interface SOC drastically enhances H_{c2}.[12]

Electron-doped $SrTiO_3$ has attracted much attention as a low-density bulk superconductor[13] with high mobility.[14] These characteristics enable the creation of novel low-dimensional systems,[15] and are vital to shed light on the rich physics present at the $LaAlO_3/SrTiO_3$ (LAO/STO) interface, where the presence of the Rashba spin-orbit interaction has been discussed, affecting both the normal- and superconducting-state transport properties.[16,17] However, despite the fact that the conduction band structure of STO is similar to the GaAs valence band,[18,19] the latter a model system for spintronics, the role of possible intrinsic SOC in the transport properties of doped STO is still unclear.

In this work, we study the violation of the superconducting Pauli limit due to intrinsic SOC in a systematic series of symmetric, doped STO heterostructures. Using the δ-doping technique, we selectively add Nb dopants in a narrow region inside an otherwise continuous undoped STO host crystal. As the thickness of the dopant layer is reduced, the destruction of superconductivity by orbital pair breaking is geometrically suppressed, and the superconducting H_{c2} is enhanced for magnetic fields applied parallel to the dopant plane. In the thin regime, when the dopant layer is just a few nanometers thick, the superconductivity is robust beyond the conventional Pauli limit, demonstrating the presence of spin-orbit scattering (SOS) in the STO. The SOS and the transport scattering times estimated from a Werthamer-Helfand-Hohenberg (WHH) theory fit demonstrate a distinct thickness dependence from that expected for the common spin scattering mechanisms. From the fact that the scattering length does not change as the doped layer thickness decreases, due to the absence of a surface or interface close to the dopant plane, as well as the lack of the Rashba effect due to the inversion-symmetric structure, we conclude that this result originates from the intrinsic SOC of STO.

The samples were fabricated with various thicknesses of 1 at. % doped Nb:$SrTiO_3$ (NSTO) films embedded between cap and buffer layers of undoped STO, using pulsed laser deposition. High-temperature growth, above ∼1050 °C, in a low oxygen partial pressure of less than 10^{-7} Torr was chosen to achieve high-quality STO films, by managing the defect chemistry of the strontium and oxygen vacancies.[20] On a TiO_2-terminated STO (100) substrate, a 100 nm undoped STO buffer layer was first grown, followed by the 1 at. % NSTO layer with various thicknesses in the range $3.9 \leqslant d \leqslant 457$ nm. A 100 nm undoped STO cap layer was grown above the doped layer, to prevent surface depletion.[21] Postannealing in a moderate oxidizing condition was used to fill oxygen vacancies formed during growth. Transport measurements were made using a standard four-probe method with sample cooling achieved using a dilution refrigerator with an *in situ* rotator. For zero-field measurements, the residual magnetic field was reduced below an absolute value of $\mu_0 H = 0.1$ mT, where μ_0 is the vacuum permeability.

All samples were superconducting at low temperatures, as shown in Fig. 1(a). The transition temperatures T_c, defined by the temperature below which the resistance was 50% of the normal-state value, were in the range $253 \leqslant T_c \leqslant 374$ mK, as shown in Fig. 1(b). All samples, except for the two thinnest, showed sharp 10%–90% transition widths (∼10 mK). While samples with thickness $d \geqslant 8.8$ nm showed relatively constant T_c (∼260 mK), several thinner samples showed a higher T_c while maintaining a sharp transition, suggesting possible changes to the superconducting properties close to the two-dimensional (2D) limit. The transition broadening in some of the thinner samples may be explained either by inhomogeneity[22] or by the Bose metal phase between the superconducting and insulating states.[23]

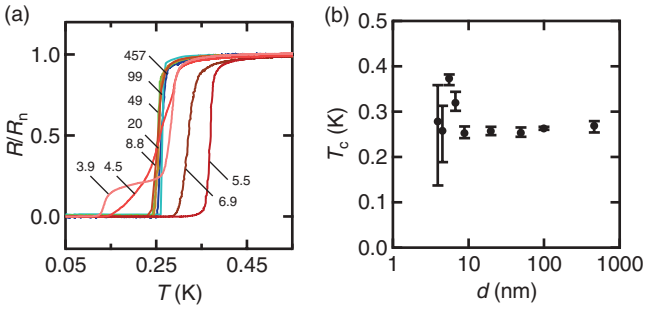

FIG. 1. (Color online) (a) Sheet resistance R, normalized by the normal-state value R_n as a function of temperature T. Numbers refer to the δ-doped layer thickness d in nanometers. (b) Superconducting transition temperature T_c versus d. T_c is defined by the temperature at the half value of the normal-state resistance; the 10%–90% width of the superconducting transition is shown as an error bar.

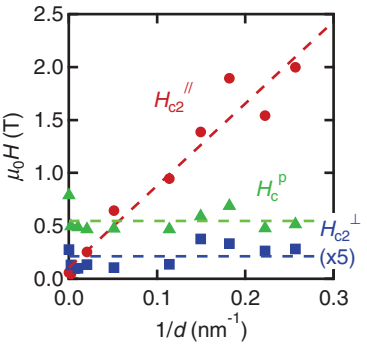

FIG. 3. (Color online) $H_{c2}^{\parallel}$ (circles), $H_{c2}^{\perp}$ (squares, scaled by a factor of 5), and the Pauli paramagnetic limit H_c^p (triangles) plotted vs $1/d$. $H_{c2}^{\parallel}$ and $H_{c2}^{\perp}$ are measured at $T = 50$ mK data. Dashed lines are guides to the eye.

First, the anisotropy of H_{c2} was used to measure the dimensionality of the superconductivity. We investigated the variation of H_{c2} by rotating the sample with respect to the magnetic field, as shown in Fig. 2(a). A bulk 1 at. % NSTO substrate was also measured as a reference. As d decreased, a clear modulation of H_{c2} as a function of the angle θ between the magnetic field and the sample plane was found. Here H_{c2} was defined as the field at which the resistance was half that of the normal state. For samples with $d \leqslant 99$ nm, excellent fits to these data could be made using Tinkham's model,[24] which is valid when the superconducting thickness is less than the Ginzburg-Landau coherence length $d_{\text{Tinkham}} < \xi_{GL}(0)$ (see Appendix A). These fits are shown in Fig. 2(a).

The dimensional crossover of superconductivity is more clearly demonstrated by the temperature dependence of H_{c2}; therefore we next measured $H_{c2}^{\perp}(t)$ and $H_{c2}^{\parallel}(t)$, the out-of-plane ($\theta = 90°$) and in-plane ($\theta = 0°$) upper critical fields, respectively (here $t = T/T_c$), as shown in Figs. 2(b) and 2(c). In the perpendicular field geometry, all samples showed a linear temperature dependence. In the parallel field geometry, however, for $d \leqslant 99$ nm, $H_{c2}^{\parallel}(t)$ showed a clear square-root form, which is characteristic of the 2D superconducting state. These data clearly demonstrate a three-dimensional (3D) to 2D crossover of the superconducting character as a function of d. By estimating d_{Tinkham} and $\xi_{GL}(0)$ from the $H_{c2}^{\perp}$ and $H_{c2}^{\parallel}$ data, we find that d_{Tinkham} decreases in proportion to the growth thickness d, and in the thinnest sample is much smaller than $\xi_{GL}(0) \approx 100$ nm, as plotted in Fig. 2(d), confirming the 2D nature of the superconductivity.

A crucial and intriguing aspect of the $H_{c2}^{\parallel}(t)$ data is the violation of the Pauli paramagnetic limit. The Pauli paramagnetic limiting field[8,9] is given by $H_c^p = \Delta_0/\sqrt{2}\mu_B$, where μ_B is the Bohr magneton (with a g factor of 2), and $\Delta_0 = 1.76 k_B T_c$ is the BCS superconducting gap for a weak-coupling superconductor, where k_B is Boltzmann's constant. This limit is appropriate, since via tunneling bulk doped STO is known to be in the weak-coupling regime.[25] The variation of $H_{c2}^{\perp}$, $H_{c2}^{\parallel}$, and H_c^p as a function of $1/d$ is shown in Fig. 3. $H_{c2}^{\parallel}$ exceeds the Pauli limiting field H_c^p by a factor of more than 4 in the thinnest sample, while $H_{c2}^{\perp}$ and H_c^p remained essentially constant.

In the case of a 2D superconductor in a parallel magnetic field, if the sample is thin enough that orbital depairing is suppressed, spin paramagnetism is the dominant mechanism for destroying superconductivity.[11] In the presence of SOS, however, $H_{c2}^{\parallel}$ can be robust beyond the Pauli limit because spin is no longer a good quantum number. It should be noted that the renormalization of normal-state properties by

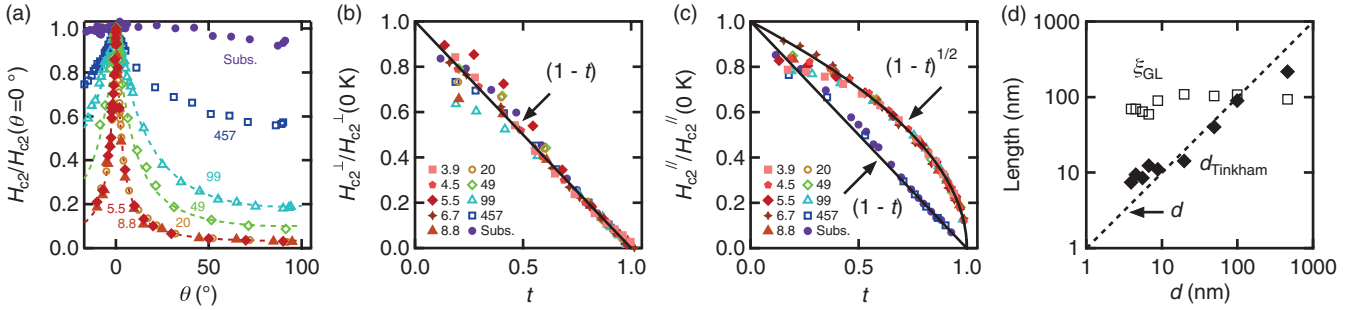

FIG. 2. (Color online) (a) Angular dependence of the upper critical field H_{c2} at $T = 50$ mK, normalized by the value at $\theta = 0°$. Dashed curves are fits to Tinkham's model. Results for representative samples (numbers refer to d in nanometers) and a bulk 1 at. % NSTO substrate (Subs.) are shown. (b) Normalized perpendicular upper critical field $H_{c2}^{\perp}/H_{c2}^{\perp}(0\text{ K})$ plotted as a function of the reduced temperature $t = T/T_c$, for all samples. $H_{c2}^{\perp}(0\text{ K})$ was obtained by extrapolation to $T = 0$ K from a fitting to the data in (b) over the range of $0.7 \leqslant t \leqslant 1$. (c) Normalized parallel upper critical field data, and fits using the same fitting procedure. (d) Ginzburg-Landau coherence length ξ_{GL} (open rectangles) and d_{Tinkham} (closed diamonds) versus d. Dashed line is $d = d_{\text{Tinkham}}$.

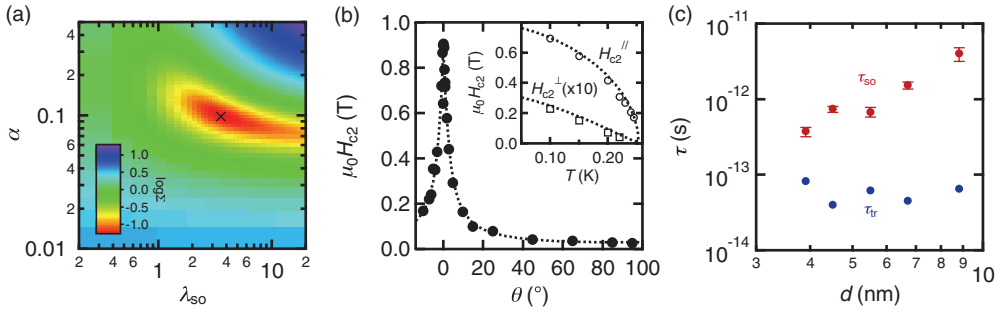

FIG. 4. (Color online) (a) Contour plot showing the deviation between the WHH simulation and the experiment by using $H_{c2}(\theta)$ data for the $d = 8.8$ nm sample. The minimum point is located at $\lambda = 3.6$, $\alpha = 9.8 \times 10^{-2}$. (b) $H_{c2}(\theta)$ of the $d = 8.8$ nm sample at $T = 50$ mK. Dotted line is the best fit obtained from the WHH simulation. Inset: $H_{c2}^{\perp}(T)$ and $H_{c2}^{\parallel}(T)$ data and the WHH theory fit (dotted line). (c) Variation of τ_{so} and τ_{tr} with d for the five thinnest samples, obtained from best fits to the WHH theory. The error bar of τ_{so} is given by assuming 10% thickness variation of the superconducting layer.

many-body effects can also enhance the Pauli limit.[26] However, Shubnikov–de Haas oscillations in these δ-doped samples showed that the electron mass is consistent with the band structure at low temperature.[15] Given the low electron density, strong correlation effects near half filling are also absent.

To investigate the effects of SOS in more detail, we performed a numerical fit of the $H_{c2}(\theta,t)$ data to the WHH theory,[10] taking into account corrections for the thin-film case (see Appendix B). Within this theory, the two crucial fitting parameters, the orbital depairing parameter α and the SOS rate λ_{so}, are given by

$$\alpha = \frac{\hbar}{2m^* D}, \tag{1}$$

$$\lambda_{so} = \frac{2\hbar}{3\pi k_B T_c \tau_{so}}, \tag{2}$$

where $\hbar$ is the Planck constant divided by 2π, m^* is the effective electron mass, $D = v_F^2 \tau_{tr}/3$ is the diffusion constant, and v_F is the Fermi velocity. τ_{tr} and τ_{so} are, respectively, the transport and SOS times. For various α and λ_{so}, we calculated the sum of the squares of the differences between the WHH model and the $H_{c2}(\theta)$ data (we denote this sum as Σ), for the case $d = 8.8$ nm, as shown in Fig. 4(a). A unique minimum value of Σ was found, giving an excellent fit to the experimental data, as shown in Fig. 4(b). A similar analysis was performed on data for the other samples where $H_{c2}^{\parallel}$ exceeded H_c^p. We obtain, for example, $\tau_{tr} = 8.3 \times 10^{-14}$ s and $\tau_{so} = 3.8 \times 10^{-13}$ s from α and λ_{so}, respectively, for $d = 3.9$ nm. This clearly indicates that the SOS is a highly significant contribution to the total scattering rate, in spite of its relatively small absolute value compared to conventional metal films.[10–12]

A crucial aspect of these SOS data is revealed by the thickness dependences of τ_{so} and τ_{tr}, as shown in Fig. 4(c). A clear decrease of τ_{so} with decreasing d is found, while τ_{tr} is relatively unchanged. This dependence suggests that the SOS is not dominated by either the Elliott-Yafet mechanism where $\tau_{so} \propto \tau_{tr}$, or the D'yakonov-Perel' mechanism where $\tau_{so} \propto 1/\tau_{tr}$.[27] This rather unexpected result suggests that the SOS observed has a different origin.

We next clarify a possible mechanism for the observed SOS by comparison with other systems. It should be emphasized here that this combination of SOC with high-mobility conduction electrons places our system in a different regime compared to other thin-film superconductors that violate the Pauli limit. For example, the use of heavy atoms to induce SOC in superconducting bilayers has been studied.[12] However, in this case, as is usual for conventional superconducting thin films, the mean free path collapses in the thin limit. A similar collapse occurs with substrate gating at the LAO/STO heterointerface[28] where an asymmetric confining potential and Rashba SOC are expected.[16,17] δ-doping is a crucial determinant for this difference: since there is no obvious surface or interface surrounding the conducting layer, the scattering length due to disorder is unchanged (and even increased) with decreasing d.[29] Additionally, the symmetry of the structure, giving rise to zero net effective electric field, means that Rashba SOC is absent.

We can thus interpret this as intrinsic SOC of STO, due to the d orbitals of the Ti atoms.[18] Indeed the bulk conduction bands of STO have a similar structure to the valence bands of GaAs, where nonperturbatively large SOC has been demonstrated.[19] However, in the case of STO there are few studies of electron SOC. It should be noted that calculations indicate that these confined δ-doped samples have a multiple-subband structure;[15] therefore the change of τ_{so} observed may relate to intersubband-induced spin-orbit interaction,[30] or intersubband scattering,[31] causing nontrivial change in both the transport and SOS times.

The fact that the energy scale of the observed SOC ($\sim$2 meV) is bigger than the superconducting gap ($\sim$40 μeV) suggests the possibility of mixed spin-triplet and -singlet states, giving rise to novel superconducting states in these low-dimensional layers.[6,7,32,33] In the normal state, we also expect that the SOS should make an important contribution to the transport properties; specifically 2D weak antilocalization (WAL) would be expected, as found in studies of SOC in metal thin films.[34] Preliminary studies have indeed observed clear 2D WAL,[35] suggesting that the combination of high-mobility electrons and SOC in STO can be employed in spintronic architectures, which can be made over a range of densities via both growth control[36] and field-effect gating, the latter simultaneously introducing Rashba contributions to the SOC.[37]

The authors thank M. Lippmaa for experimental assistance and M. R. Beasley, A. Bhattacharya, N. Breznay,

A. Kapitulnik, K. H. Kim, A. H. MacDonald, A. F. Morpurgo, A. Palevski, B. Spivak, and H. Takagi for discussions. M.K., C.B., Y.H., and H.Y.H. acknowledge support by the Department of Energy, Office of Basic Energy Sciences, Materials Sciences and Engineering Division, under Contract No. DE-AC02-76SF00515. M.K. acknowledges support from the Japanese Government Scholarship Program of the Ministry of Education, Culture, Sport, Science and Technology, Japan.

APPENDIX A: TINKHAM'S MODEL

The magnetic-field response of a two-dimensional superconductor can be described by Tinkham's model,[24] which assumes that the superconductor is thinner than the Ginzburg-Landau coherence length, $d_{\mathrm{Tinkham}} < \xi_{\mathrm{GL}}$. It should be noted that the model does not include the effects of SOS or the Pauli paramagnetic limit, and assumes an isotropic superconducting wave function. According to the model, the angular dependence of the upper critical field can be shown to be

$$\left|\frac{H_{c2}(\theta)\sin\theta}{H_{c2}^{\perp}}\right| + \left(\frac{H_{c2}(\theta)\cos\theta}{H_{c2}^{\parallel}}\right)^2 = 1, \tag{A1}$$

where θ is the angle between the magnetic field and the sample plane. The temperature dependence of the upper critical field in perpendicular and parallel field geometry is given by

$$H_{c2}^{\perp}(t) = \frac{\Phi_0}{2\pi\xi_{\mathrm{GL}}(0)^2}(1-t), \tag{A2}$$

$$H_{c2}^{\parallel}(t) = \frac{\Phi_0\sqrt{12}}{2\pi\xi_{\mathrm{GL}}(0)d_{\mathrm{Tinkham}}}(1-t)^{1/2}, \tag{A3}$$

where $t = T/T_c$ is the reduced temperature, $\Phi_0 = h/2e = 2.07\times10^{-15}$ Wb is the flux quantum, and $\xi_{\mathrm{GL}}(0)$ is the Ginzburg-Landau coherence length extrapolated to $T = 0$ K. From Eqs. (A2) and (A3), d_{Tinkham} and $\xi_{\mathrm{GL}}(0)$ can be found using

$$d_{\mathrm{Tinkham}} = \sqrt{\frac{6\Phi_0 H_{c2}^{\perp}}{\pi(H_{c2}^{\parallel})^2}}, \tag{A4}$$

$$\xi_{\mathrm{GL}}(0) = \sqrt{\frac{\Phi_0}{2\pi H_{c2}^{\perp}}}. \tag{A5}$$

Thus, d_{Tinkham} can be calculated by measurement of $H_{c2}^{\perp}$ and $H_{c2}^{\parallel}$ of a sample experimentally. As noted by Ben Shalom *et al.*,[17] in the case of the $LaAlO_3/SrTiO_3$ interface, the value of d_{Tinkham} is an upper bound on the thickness. In our case we find good agreement between the grown dopant layer thickness d and d_{Tinkham} in thick samples, but d_{Tinkham} deviates slightly from d as $H_{c2}^{\parallel}$ exceeds the Pauli limiting field in the thinnest samples ($d \leqslant 8.8$ nm), possibly indicating a limit of the model.

APPENDIX B: WHH THEORY

The Werthamer-Helfand-Hohenberg theory[10] was used to more quantitatively fit the data for the superconducting upper critical field H_{c2} in the main text, in order to determine the SOS time in the system. Within this theory H_{c2} is the implicit solution of the equation

$$\ln t + \left(\frac{1}{2} + \frac{i\lambda_{\mathrm{so}}}{4\gamma}\right)\psi\left(\frac{1}{2} + \frac{\bar{h} + \frac{1}{2}\lambda_{\mathrm{so}} + i\gamma}{2t}\right) + \left(\frac{1}{2} - \frac{i\lambda_{\mathrm{so}}}{4\gamma}\right)\psi\left(\frac{1}{2} + \frac{\bar{h} + \frac{1}{2}\lambda_{\mathrm{so}} - i\gamma}{2t}\right) - \psi\left(\frac{1}{2}\right) = 0, \tag{B1}$$

where ψ is the digamma function. With a slight correction[38] from the original WHH paper, the terms are defined as

$$\bar{h} = \frac{DeH_{c2}}{\pi k_B T_c}, \tag{B2}$$

$$\lambda_{\mathrm{so}} = \frac{2\hbar}{3\pi k_B T_c \tau_{\mathrm{so}}}, \tag{B3}$$

$$\gamma = \sqrt{(\alpha\bar{h})^2 - \frac{1}{4}\lambda_{\mathrm{so}}^2}, \tag{B4}$$

$$\alpha = \frac{\hbar}{2mD}, \tag{B5}$$

where D is the diffusion constant, τ_{so} the SOS time, and m the electron mass. To include the effect of the finite thickness of a thin film, the term $\bar{h}$ in Eq. (B1) should be replaced by $\bar{h}^{\mathrm{ang}}(\theta)$, which is given by[39]

$$\bar{h}^{\mathrm{ang}}(\theta) = \frac{D}{2\pi k_B T_c}\left(2eH_{c2}|\sin(\theta)| + \frac{1}{3\hbar}[deH_{c2}\cos(\theta)]^2\right), \tag{B6}$$

where d is the thickness of the superconducting layer.

In the case of $\alpha = \lambda_{\mathrm{so}} = 0$ (no SOS, but also no Pauli paramagnetic limit), the above formula is reduced to the orbital term only, where H_{c2} is the solution of

$$\ln t + \psi\left(\frac{1}{2} + \frac{\bar{h}}{2t}\right) - \psi\left(\frac{1}{2}\right) = 0. \tag{B7}$$

In fitting the data, the orbital-only case [Eq. (B7)] could not accurately fit the data for samples with $H_{c2}^{\parallel}$ larger than the Pauli paramagnetic limit (not shown). However, we could obtain a very successful fit with the full WHH theory [Eq. (B1)], as discussed and shown in the main text (Fig. 4).

Several sources of error should be considered in this fit. First, it has been argued that cooling superconducting ultrathin

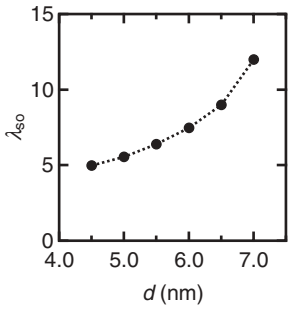

FIG. 5. Optimal value of λ_{so} from the WHH fitting for the $d = 5.5$ nm sample, depending on the thickness d used in the model.

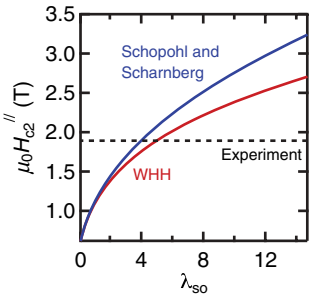

FIG. 6. (Color online) Variation of $H_{c2}^{\parallel}$ with λ_{so} using a nonperturbative spin-orbit coupling model, compared to the original WHH model, adapted from Schopohl and Scharnberg (Ref. 41). The $d = 5.5$ nm sample was used.

films below 60 mK is extremely difficult;[40] thus the $H_{c2}(t)$ data may artificially saturate at low temperatures due to a lack of cooling. However, by fitting to data at temperatures only above 75 mK, we find an increase of the value of τ_{so} of only 2% compared to the full fitting curve. Second, the influence of error in the value of d used in Eq. (B6) can also be considered. This effect is demonstrated in Fig. 5, where the value of τ_{so} obtained from the fitting is plotted against d for the $d = 5.5$ nm sample. As is clear, sensitivity of the fit to variation in d gives rise to variation in τ_{so}; we obtain $\tau_{so} = (6.8 \pm 1.0) \times 10^{-13}$ s for $d = 5.5 \pm 0.5$ nm.

We note that the WHH theory makes various simplifying assumptions: The superconductor should be in the dirty limit, where the electron mean free path is shorter than the BCS coherence length $\ell \ll \xi_{BCS}$. Second, the SOS time is much larger than the transport scattering time, $\tau_{so} \gg \tau_{tr}$. In order to estimate these parameters, we assume a single-band approximation with spherical Fermi surface and used an electron effective mass $m^* = 1.24m_0$, where m_0 is the bare electron mass, extracted from Shubnikov–de Haas oscillations.[15] In the $d = 5.5$ nm sample, for instance, we found $\ell \approx 100$ nm, $\xi_{BCS} \approx 470$ nm. From the WHH fit, we estimated $\tau_{so} \approx 6.8 \times 10^{-13}$ s and $\tau_{tr} \approx 6.2 \times 10^{-14}$ s. Therefore, we conclude that our system is in the dirty limit, and SOC can be treated as a perturbation. The latter, however, becomes less clear with decreasing thickness, for which $\tau_{tr}/\tau_{so} \approx 0.1$. As a further check, we used a nonperturbative theory proposed by Schopohl and Scharnberg.[41] The value of $H_{c2}^{\parallel}$ for various λ_{so} using this theory is shown in Fig. 6, along with the original WHH model (neglecting the finite-size corrections of Aoi *et al.*[39]). Since in absolute terms the observed values of $H_{c2}^{\parallel}$ are not large due to the relatively low T_c, we estimate an error of only ~20% in the determination of τ_{so} by using the original WHH model, as shown, which does not significantly affect the result of the original fitting.

[1] M. Sigrist and K. Ueda, Rev. Mod. Phys. **63**, 239 (1991).
[2] P. Fulde and R. A. Ferrell, Phys. Rev. **135**, A550 (1964).
[3] A. I. Larkin and Y. N. Ovchinnikov, Zh. Eksp. Teor. Fiz. **47**, 1136 (1964) [Sov. Phys. JETP **20**, 762 (1965)].
[4] A. P. Mackenzie and Y. Maeno, Rev. Mod. Phys. **75**, 657 (2003).
[5] E. Bauer, G. Hilscher, H. Michor, C. Paul, E. W. Scheidt, A. Gribanov, Y. Seropegin, H. Noel, M. Sigrist, and P. Rogl, Phys. Rev. Lett. **92**, 027003 (2004).
[6] L. P. Gor'kov and E. I. Rashba, Phys. Rev. Lett. **87**, 037004 (2001).
[7] S. K. Yip, Phys. Rev. B **65**, 144508 (2002).
[8] B. S. Chandrasekhar, Appl. Phys. Lett. **1**, 7 (1962).
[9] A. M. Clogston, Phys. Rev. Lett. **9**, 266 (1962).
[10] N. R. Werthamer, E. Helfand, and P. C. Hohenberg, Phys. Rev. **147**, 295 (1966).
[11] P. M. Tedrow and R. Meservey, Phys. Rev. B **8**, 5098 (1973).
[12] X. S. Wu, P.W. Adams, Y. Yang, and R. L. McCarley, Phys. Rev. Lett. **96**, 127002 (2006).
[13] C. S. Koonce, M. L. Cohen, J. F. Schooley, W. R. Hosler, and E. R. Pfeiffer, Phys. Rev. **163**, 380 (1967).
[14] O. N. Tufte and P. W. Chapman, Phys. Rev. **155**, 796 (1967).
[15] Y. Kozuka, M. Kim, C. Bell, B. G. Kim, Y. Hikita, and H. Y. Hwang, Nature (London) **462**, 487 (2009).
[16] A. D. Caviglia, M. Gabay, S. Gariglio, N. Reyren, C. Cancellieri, and J. M. Triscone, Phys. Rev. Lett. **104**, 126803 (2010).
[17] M. Ben Shalom, M. Sachs, D. Rakhmilevitch, A. Palevski, and Y. Dagan, Phys. Rev. Lett. **104**, 126802 (2010).
[18] L. F. Mattheiss, Phys. Rev. B **6**, 4718 (1972).
[19] B. Grbic, R. Leturcq, T. Ihn, K. Ensslin, D. Reuter, and A. D. Wieck, Phys. Rev. B **77**, 125312 (2008).
[20] Y. Kozuka, Y. Hikita, C. Bell, and H. Y. Hwang, Appl. Phys. Lett. **97**, 012107 (2010).
[21] A. Ohtomo and H. Y. Hwang, Appl. Phys. Lett. **84**, 1716 (2004).
[22] O. Foyevtsov, F. Porrati, and M. Huth, Phys. Rev. B **84**, 045103 (2011).
[23] N. Mason and A. Kapitulnik, Phys. Rev. Lett. **82**, 5341 (1999).
[24] M. Tinkham, Phys. Rev. **129**, 2413 (1963).
[25] G. Binnig and H. E. Hoenig, Solid State Commun. **14**, 597 (1974).
[26] T. P. Orlando, E. J. McNiff, S. Foner, and M. R. Beasley, Phys. Rev. B **19**, 4545 (1979).
[27] I. Žutić, J. Fabian, and S. Das Sarma, Rev. Mod. Phys. **76**, 323 (2004).
[28] C. Bell, S. Harashima, Y. Kozuka, M. Kim, B. G. Kim, Y. Hikita, and H. Y. Hwang, Phys. Rev. Lett. **103**, 226802 (2009).
[29] Y. Kozuka, M. Kim. H. Ohta, Y. Hikita, C. Bell, and H. Y. Hwang, Appl. Phys. Lett. **97**, 222115 (2010).
[30] E. Bernardes, J. Schliemann, M. Lee, J. C. Egues, and D. Loss, Phys. Rev. Lett. **99**, 076603 (2007).
[31] J. E. Hansen, R. Taboryski, and P. E. Lindelof, Phys. Rev. B **47**, 16040 (1993).
[32] V. L. Ginzburg, Phys. Lett. **13**, 101 (1964).
[33] K. Michaeli, A. C. Potter, and P. A. Lee, Phys. Rev. Lett. **108**, 117003 (2012).
[34] G. Bergmann, Phys. Rev. Lett. **48**, 1046 (1982).
[35] M. Kim *et al.* (unpublished).

[36]M. Kim, C. Bell, Y. Kozuka, M. Kurita, Y. Hikita, and H. Y. Hwang, Phys. Rev. Lett. **107**, 106801 (2011).
[37]T. Koga, J. Nitta, T. Akazaki, and H. Takayanagi, Phys. Rev. Lett. **89**, 046801 (2002).
[38]A. L. Fetter and P. C. Hohenberg in *Superconductivity*, edited by R. D. Parks (Marcel Dekker, New York, 1969).
[39]K. Aoi, R. Meservey, and P. M. Tedrow, Phys. Rev. B **7**, 554 (1973).
[40]K. A. Parendo, K. H. Sarwa B. Tan, and A. M. Goldman, Phys. Rev. B **73**, 174527 (2006).
[41]N. Schopohl and K. Scharnberg, Physica B&C **107**, 293 (1981).